THE JOURNAL OF BIOLOGICAL CHEMISTRY
Vol. 274, No. 34, Issue of August 20, pp. 24100–24112, 1999
Printed in U.S.A.

Mutational Analysis of the Tetrahydrobiopterin-binding Site in Inducible Nitric-oxide Synthase*

(Received for publication, March 5, 1999, and in revised form, May 21, 1999)

Sanjay Ghosh‡, Dennis Wolan‡, Subrata Adak‡, Brian R. Crane§, Nyoun Soo Kwon¶, John A. Tainer§, Elizabeth D. Getzoff§, and Dennis J. Stuehr‡‖

From the ‡Department of Immunology, Lerner Research Institute, Cleveland Clinic, Cleveland, Ohio 44195, §Department of Molecular Biology, The Skaggs Institute for Chemical Biology, Scripps Research Institute, La Jolla, California 92037, and the ¶Department of Biochemistry, Chung-Ang Medical School, Seoul 156-756, Korea

Inducible nitric-oxide synthase (iNOS) is a hemeprotein that requires tetrahydrobiopterin (H4B) for activity. The influence of H4B on iNOS structure-function is complex, and its exact role in nitric oxide (NO) synthesis is unknown. Crystal structures of the mouse iNOS oxygenase domain (iNOSox) revealed a unique H4B-binding site with a high degree of aromatic character located in the dimer interface and near the heme. Four conserved residues (Arg-375, Trp-455, Trp-457, and Phe-470) engage in hydrogen bonding or aromatic stacking interactions with the H4B ring. We utilized point mutagenesis to investigate how each residue modulates H4B function. All mutants contained heme ligated to Cys-194 indicating no deleterious effect on general protein structure. Ala mutants were monomers except for W457A and did not form a homodimer with excess H4B and Arg. However, they did form heterodimers when paired with a full-length iNOS subunit, and these were either fully or partially active regarding NO synthesis, indicating that preserving residue identities or aromatic character is not essential for H4B binding or activity. Aromatic substitution at Trp-455 or Trp-457 generated monomers that could dimerize with H4B and Arg. These mutants bound Arg and H4B with near normal affinity, but Arg could not displace heme-bound imidazole, and they had NO synthesis activities lower than wild-type in both homodimeric and heterodimeric settings. Aromatic substitution at Phe-470 had no significant effects. Together, our work shows how hydrogen bonding and aromatic stacking interactions of Arg-375, Trp-457, Trp-455, and Phe-470 influence iNOSox dimeric structure, heme environment, and NO synthesis and thus help modulate the multiple effects of H4B.

Nitric oxide (NO)[1] is produced by many cells and plays important roles in the nervous, muscular, cardiovascular, and immune systems (1–5). Neuronal NOS (nNOS, NOS 1) and endothelial NOS (eNOS, NOS 3) produce low NO concentrations for neurotransmission, insulin release, penile erection, vasorelaxation, oxygen detection, and memory storage, whereas cytokine-inducible NOS (iNOS, NOS 2) produces larger NO concentrations to counter pathogens and coordinate the immune response. The iNOS binds calmodulin (CaM) very tightly and is not regulated by changes in intracellular Ca^{2+}, whereas the eNOS and nNOS isoforms both bind CaM reversibly and are regulated by intracellular Ca^{2+} (6–8).

All three NOS exhibit a similar catalytic profile and composition. They catalyze a two-step oxidation of L-arginine (Arg) to form NO and citrulline, with *N*-hydroxy-L-arginine (NOHA) being formed as an enzyme-bound intermediate (9–11). The amino-terminal portion of each NOS represents an oxygenase domain (amino acids 1–498 in mouse iNOS) that binds Fe-protoporphyrin IX (heme), Arg, and (6*R*)-tetrahydrobiopterin (H4B) (12, 13). The carboxyl-terminal portion of NOS represents a reductase domain (amino acids 533–1172 in mouse iNOS) that contains binding sites for NADPH, FAD, and FMN and bears much resemblance to cytochrome P450 reductase and other homologous dual flavin enzymes (9, 11, 13). An intervening CaM-binding sequence (amino acids 503–532 for mouse iNOS) separates the two domains. Each domain has distinct roles in catalysis and in forming the active dimeric structure (12). For example, the iNOS reductase domains, which do not appear to participate in the dimeric interaction, transfer NADPH-derived electrons to the heme irons in the oxygenase domain dimer, which enables the hemes to bind and activate O_2 during NO synthesis (9, 11–13).

The NOS oxygenase and reductase domains can be expressed separately and fold and function independently of one another. This has facilitated spectroscopic, kinetic, mutagenic, and crystallographic analysis of the mouse iNOS oxygenase domain (iNOSox) (14–19). Mouse iNOSox that is overexpressed in bacteria is primarily dimeric as purified and can bind Arg and H4B with normal affinity. Moreover, iNOSox can synthesize NO from the reaction intermediate NOHA when reducing equivalents are provided by either free reductase domains (20) or dithionite[2] and also can synthesize nitrite from NOHA in a H_2O_2-supported reaction (17, 21). Both full-length iNOS and iNOSox dimers can reversibly dissociate into folded, heme-containing monomers in the presence of urea (12). These full-length and iNOSox monomers recombine with one another when H4B and Arg are present to form stable iNOS heterodimers (22). Because such heterodimers contain only one reductase domain, they have been useful in dissecting the electron transfer pathway in iNOS. For example, iNOS het-

* This work was supported by National Institutes of Health Grants CA53914 and HL58883. The costs of publication of this article were defrayed in part by the payment of page charges. This article must therefore be hereby marked "*advertisement*" in accordance with 18 U.S.C. Section 1734 solely to indicate this fact.

‖ To whom correspondence should be addressed: Immunology NN-1, Lerner Research Institute, Cleveland Clinic, 9500 Euclid Ave., Cleveland, OH 44195. Tel.: 216-445-6950; Fax: 216-444-9329; E-mail: stuehrd@cesmtp.ccf.org.

[1] The abbreviations used are: NO, nitric oxide; NOS, NO synthase; Arg, L-arginine; H4B (6*R*)-5,6,7,8-tetrahydro-L-biopterin; BME, β-mercaptoethanol; CaM, calmodulin; BSA, bovine serum albumin; DTT, dithiothreitol; EPPS, 4-(2-hydroxyethyl)-1-piperazinepropanesulfonic acid; H_2O_2, hydrogen peroxide; iNOS, mouse macrophage inducible NO synthase; iNOSox, oxygenase domain of iNOS; NOHA, N^{ω}-hydroxy-L-arginine; eNOS, endothelial NOS; nNOS, neuronal NOS.

[2] S. Boggs, L. Huang, H. Abu-Soud, and D. J. Stuehr, unpublished results.

erodimers containing an Arg-binding mutation were used to show that flavin-to-heme electron transfer in an iNOS dimer occurs exclusively between reductase and oxygenase domains of adjacent subunits (23). Besides providing one reason why dimerization is critical for NO synthesis, this work also showed how heterodimers can help investigate whether single mutations affect iNOS structure-function in a dimeric setting.

Determining how H4B functions in NOS catalysis is key to understanding the enzyme reaction mechanism. Recently solved crystal structures for iNOSox and the eNOS oxygenase domain dimers (19, 24) show that H4B is positioned perpendicular to the heme plane and at such a distance from bound substrate that it cannot participate directly in oxygen activation reactions critical for NO synthesis. This is consistent with a variety of biochemical and kinetic evidence that indicates H4B has important structural and electronic effects in iNOS. For example, H4B promotes dimer assembly of iNOS heme-containing monomers (25), protects against proteolysis at Lys-117 in the amino-terminal hook (17), slows CO binding by 100-fold (14), prevents binding of bulky ligands such as DTT (17) or nitrosoalkanes (26) to the heme, and increases Arg binding affinity (27). Electronic effects include H4B causing a high spin shift of the heme iron (21, 27–28), increasing the heme midpoint potential (29), stabilizing the Fe-S bond in ferrous-CO or -NO complexes (14, 30), and increasing the reactivity of the ferrous-O_2 complex 70-fold.[3] Many of these effects have also been observed in nNOS or eNOS. In particular, H4B helps stabilize the nNOS dimer (31), increases the reactivity of its ferrous-O_2 complex (32), and has been suggested to act as an electron donor under certain circumstances during NO synthesis (33). However, there also appear to be differences among the NOS particularly regarding a role for H4B in promoting dimer formation (24, 34).

Recent work has examined how various structural components of H4B and its ring redox state help promote the H4B-induced effects noted above and support NO synthesis. Studies utilizing tetrahydro- and dihydropterin analogs of H4B show that whereas both the dihydroxypropyl side chain and the pterin ring help determine binding affinity toward NOS, the side chain is more important than the ring in this regard (27, 35). Considering the pterin ring oxidation state, work with iNOS shows that dihydrobiopterin can mimic H4B in promoting all of the structural or electronic effects listed above except for increasing the reactivity of the ferrous-O_2 complex and supporting NO synthesis. This suggests an essential role for H4B is to modulate reactivity of heme iron-oxygen complexes during NO synthesis (32). In any case, protein interactions with H4B are likely to modulate many of its electronic and structural functions noted above.

From the iNOSox crystal structure it is clear that residues from both the amino and carboxyl termini interact with H4B (19). Amino-terminal residues interact primarily with the dihydroxypropyl side chain of H4B, whereas residues in the carboxyl terminus primarily interact with the pterin ring. Four highly conserved residues that interact with the pterin ring are located in the substrate-binding helix (Arg-375) and in a helical lariat structure (Trp-455, Trp-457, and Phe-470) (Fig. 1, *A* and *B*). Each H4B interacts with two residues provided by the same subunit and two provided by the adjacent subunit of the dimer, and contact with the H4B ring occurs through π-stacking and/or hydrogen-bonding interactions (Fig. 1, *A* and *C*). Together, these four residues hold the pterin ring perpendicular to the heme plane and close enough to directly hydrogen-bond to a heme propionate through pterin N-3 (19) (Fig. 1*C*). To understand the importance of these four residues (Arg-375, Trp-455, Trp-457, and Phe-470), we employed point mutagenesis to ablate or modify their interactions with the H4B ring, and we characterized each mutant regarding dimer formation, H4B and Arg binding, and enzyme catalysis. We tested the effect of each mutant when it was present in both subunits of an iNOSox homodimer and also when it was present in only one subunit of a iNOS heterodimer comprised of an oxygenase and full-length subunit. Our results show these four residues modulate H4B function in several ways and are important determinants for controlling iNOS structure-function.

EXPERIMENTAL PROCEDURES

Materials—(6*R*)-H4B was purchased from Dr. B. Schirck's laboratory (Jona, Switzerland). ∂-Aminolevulinic acid, Arg, bovine serum albumin (BSA), L-citrulline, 4-(2-hydroxyethyl)-1-piperazinepropanesulfonic acid (EPPS), imidazole, sodium dithionite, sodium nitrite, superoxide dismutase, catalase, hydrogen peroxide were purchased from Sigma. Ampicillin and isopropyl-β-D-thiogalactopyranoside were purchased from Roche Molecular Biochemicals GmbH (Germany). NOHA was purchased from Alexis (San Diego, CA). DTT was purchased from Aldrich. Glycerol and Terrific Broth were purchased from Life Technologies, Inc. His-Bind (nitrilotriacetate) resin was purchased from Novagen (Madison, WI). Site-specific oligonucleotide-directed mutagenesis was performed using the Altered Sites II *in vitro* mutagenesis system of Promega Biochemicals. Primers were synthesized by Life Technologies, Inc.

Protein Expression and Purification—Bacterial expression and purification of the G450A full-length iNOS mutant (18) was done as reported previously for wild-type full-length iNOS (36). Wild-type and mutant iNOSox proteins (amino acids 1–498) with a His_6 tag attached to their carboxyl terminus were overexpressed in *Escherichia coli* strain BL21(DE3) using a modified pCWori vector (16). The cultures were grown with shaking at 250 rpm at 25 °C. Expression of protein was induced by adding 1 mM isopropyl-β-D-thiogalactopyranoside to the culture when it reached an optical density of 1 at 600 nm, and ∂-aminolevulinic acid was also added at this point to give a final concentration of 450 μM. Cells were harvested 48 h after induction by centrifugation at 3600 rpm for 15 min. The cells from 4 liters of culture were suspended in a minimum volume of lysis buffer containing 40 mM EPPS, pH 7.6, 0.5 mg/ml lysozyme, 10% glycerol, 0.5 μg/ml each of leupeptin, pepstatin, and phenylmethylsulfonyl fluoride, 1 mM Arg, and 0.25 M NaCl. Cells were broken by sonication (three 10-s pulses) followed by three cycles of freezing and thawing in liquid N_2 and at 37 °C, respectively. The suspension was centrifuged at 13,200 rpm for 25 min to remove cell debris, and the cytochrome P450 concentration of the supernatant was checked. The crude extract was loaded onto a Ni-nitrilotriacetate-Sepharose 4B column (2.5/10 cm) previously charged with 50 mM $NiSO_4$ and equilibrated with 40 mM EPPS buffer, pH 7.6, containing 10% glycerol, 1 mM phenylmethylsulfonyl fluoride, and 0.25 M NaCl (buffer A). The column was then washed with 10-bed volumes of buffer A and 5-bed volumes of buffer A containing 40 mM imidazole. Bound protein was eluted with buffer A containing 150–200 mM imidazole. Column fractions containing iNOSox were pooled and concentrated using a Centriprep-30 (Millipore). The concentrated proteins were dialyzed at 4 °C against two 500-ml volumes of 40 mM EPPS, pH 7.6, 10% glycerol, and 1 mM DTT and stored in aliquots at −70 °C.

Molecular Biology—Restriction digestions, cloning, bacterial growth, transformation, and isolation of DNA fragments were performed using standard procedures (37). Site-directed mutagenesis was done using the Altered Sites II *in vitro* Mutagenesis kit from Promega. Mutant cDNAs were cloned into the *Nde*I and *Sal*I sites of the pCWori vector and transformed into *E. coli* BL21(DE3) for protein expression.

UV-visible Spectroscopy—Spectral data were recorded on a Hitachi U3110 spectrophotometer in the presence or absence of H4B and Arg. Scans of dithionite-reduced CO-bound proteins were taken in 40 mM EPPS, pH 7.6, containing 10% glycerol, 1 mM DTT, 3 mM Arg, and various concentrations of H4B. The ferrous-CO adduct absorbing at 444 nm was used to quantitate the hemeprotein content using an extinction coefficient of 74 mM^{-1} cm^{-1} (A_{444}-A_{500}) (38). Spectral analysis of H4B binding was done at room temperature using protein samples that had been incubated overnight at 4 °C with various concentrations of H4B (0.1–1 mM). Proteins were diluted in 40 mM EPPS, pH 7.6, containing 5% glycerol and 3 mM DTT or 3 mM β-mercaptoethanol (BME) plus different concentrations of H4B.

Arg binding affinity was studied by perturbation difference spectroscopy according to methods described previously (39, 40). Protein samples were incubated with H4B overnight at 4 °C and then diluted to ~3

[3] H. Abu-Soud and D. J. Stuehr, unpublished results.

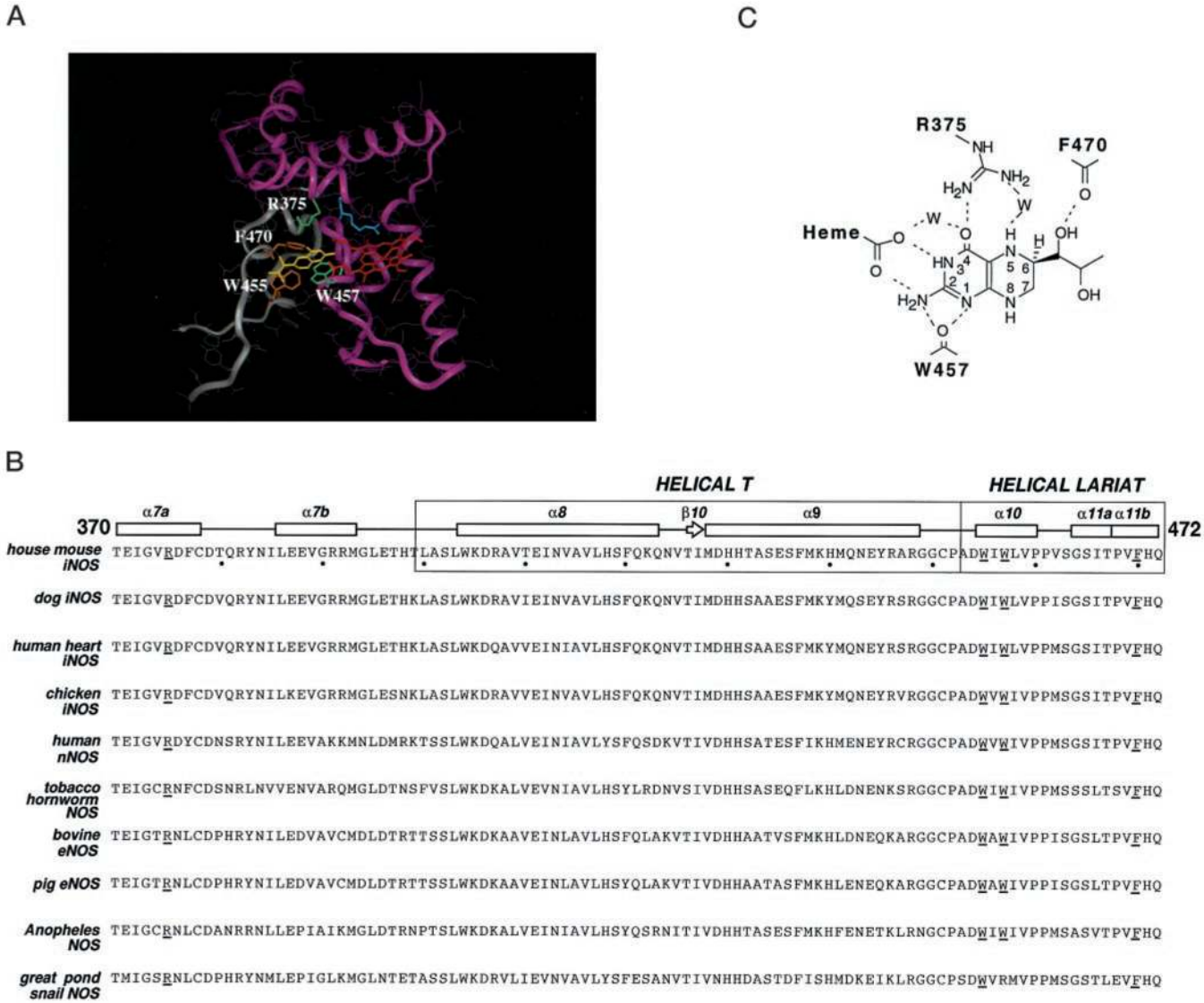

FIG. 1. **Interaction of Arg-375, Trp-455, Trp-457, and Phe-470 with H4B in an iNOSox dimer.** *A* depicts a *yellow* H4B molecule bound within the dimer interface. The *purple ribbon* structure is from the same subunit to which H4B is bound and represents residues 370–480 depicting the substrate-binding helix (providing *green* Arg-375), intervening helical T, and helical lariat (providing *green* Trp-457) (19). A *blue* Arg molecule is also shown bound to the substrate-binding helix and positioned *above* the *red* heme group contained in this subunit of the dimer. The *gray* ribbon structure is from the partner subunit and represents residues 450–475 depicting the helical lariat (providing *orange* Phe-470 and Trp-455). *B* aligns 10 NOS polypeptide sequences from diverse life forms that contain the four H4B-interacting residues, which are *underlined*. The *upper line* illustrates the secondary structural elements contained within the linear sequences. *C* illustrates hydrogen-bonding interactions (*dashed lines*) between H4B and Arg-375, Trp-457, Phe-470, and water molecules (*W*). Peptide backbone carbonyl hydrogen-bonding interactions are depicted using a carbonyl stick structure. A hydrogen-bonding interaction between H4B and a heme propionate group is also shown.

μM in buffer containing 10% glycerol, 1 mM DTT, 300 μM H4B, and 0.4 mM imidazole to promote formation of a low spin heme-imidazole complex prior to titration. Spectra were recorded after equilibrium was reached ~10 min after each addition of Arg. The final sample volume change was less than 5%. Difference spectra were generated by subtracting the spectrum obtained without Arg from each subsequent spectrum using Spectra Calc software (Galactic Industries Corp.). Apparent binding constants for Arg were determined from double-reciprocal plots of the difference in the respective peak to trough absorbances *versus* the Arg concentration. For mutants whose Arg binding affinity was determined in the presence of imidazole, we also determined their imidazole binding affinities by serially adding imidazole to a cuvette containing a mutant iNOSox, 0.5 mM H4B, but no Arg, and a spectrum was recorded after each addition. The data were analyzed by double-reciprocal plotting as described above to determine imidazole K_s values. Imidazole K_s values were then used in Equation 1 to correct for the effect of imidazole on the apparent Arg K_s values (50),

$$\text{Ks Arg} = \frac{\text{apparent } K_s \text{ Arg}}{[1 + (\text{imidazole concentration}/K_d \text{ for imidazole})]} \quad \text{(Eq. 1)}$$

Arg binding for some mutants was studied without imidazole. In this case proteins were incubated overnight at 4 °C with 1 mM H4B and then diluted in the same buffer as above containing 1 mM H4B, and the spectra were recorded after each addition of Arg and analyzed by double-reciprocal analysis.

Gel Filtration Analysis—Dimer and monomer content of iNOSox proteins was estimated by chromatography on an Amersham Pharmacia Biotech Superdex-200 HR size-exclusion column equilibrated with 40 mM EPPS, pH 7.4, containing 10% glycerol, 0.25 M NaCl, and 0.5 mM DTT. The molecular weight of the protein peaks were estimated relative to protein molecular weight standards as described previously (17, 40).

Product Formation from NOHA—Catalysis of nitrite production from NOHA and H_2O_2 by iNOSox or mutants was assayed in 96-well microplates at 37 °C as described previously (16, 41) with modifications. Assays (0.1 ml final volume) contained 100 mM EPPS, pH 7.5, 150 nM iNOSox hemeprotein, 1 mM NOHA, 0.5 mM DTT, 30 mM H_2O_2, 10 units/ml superoxide dismutase, 50 μg/ml BSA, and variable concentrations of H4B (0.3–100 μM). Reactions were started by adding H_2O_2 and stopped by adding catalase (1300 units). Griess reagent (0.1 ml) was then added, and the assay plate was read at 550 nm in a Thermomax

plate reader. Nitrite production was quantitated based on $NaNO_2$ standards.

Heterodimer Formation between iNOSox and Full-length G450A iNOS—For monomer formation, wild-type iNOSox or mutant iNOSox proteins were incubated 1.5 h at a concentration of 50–70 μM in 40 mM EPPS pH 7.6, containing 5 M urea, 3 mM DTT, and 10% glycerol at 37 °C. They were then placed on ice and incubated for an additional 30 min. The samples were then diluted 10-fold with 40 mM EPPS, 10% glycerol, and 3 mM DTT and incubated at various concentrations (0–2.5 μM) with 200 nM full-length G450A monomer for complementation experiments. Antagonist experiments were done the same way except they also included 300 nM wild-type iNOSox monomer in each well. To promote dimerization 1 mM BH_4 and 20 mM Arg were added to the protein mixtures to give a final volume of 50 μl, and the samples were incubated for 1 h at 30 °C. For antagonist experiments, protein mixtures were preincubated for 30 min prior to adding H4B and Arg. After this dimerization incubation, heterodimer NO synthesis was assayed by diluting each sample to 100 μl with assay buffer such that each well contained a final concentration of 40 mM EPPS, 3 mM DTT, 4 μM FAD, 4 μM FMN, 800 μM H4B, 15 mM Arg, 1 mg/ml BSA, 18 units/ml catalase, and 10 units/ml superoxide dismutase. NADPH (1 mM) was added to start the NO synthesis reaction. The assays ran for 1 h at 37 °C, and the reactions stopped by enzymatic oxidation of NADPH. Griess reagent (0.1 ml) was added to each well, and the absorbance was measured at 550–650 nm in a microplate reader. Absorbance due to nitrite produced in the reaction was quantitated based on $NaNO_2$ standards.

In some cases heterodimer NO synthesis was assayed using the spectrophotometric oxyhemoglobin assay (23, 35). After the dimerization incubation, sample aliquots were transferred from the microwells into cuvettes containing 40 mM EPPS, pH 7.6, 10 mM Arg, 0.1 mM H4B, 0.3 mM DTT, 1 mg/ml BSA, 10 units/ml superoxide dismutase, 100 units/ml catalase, 4 μM FAD and FMN, 5 μM oxyhemoglobin, and 300 μM NADPH in a total reaction volume of 500 μl. Heterodimer concentrations ranged from 10 to 30 nM in the cuvette, and the reactions were started by adding NADPH and run at 37 °C. The NO-mediated conversion of oxyhemoglobin to methemoglobin over the first 5 min of the reaction was monitored at 401 nm and converted to a rate of NO synthesis using the difference extinction coefficient of $\epsilon_{401} = 38\ mM^{-1}\ cm^{-1}$.

RESULTS

All nine mutant iNOSox proteins were purified in the absence of Arg and H4B. The amount of recoverable protein varied from 5 to 15 mg/liter culture, and all purified proteins displayed a normal heme content and molecular mass (data not shown). Their dithionite-reduced, CO-bound forms all displayed a Soret peak at 444 nm, indicating that the heme iron in each mutant is ligated to Cys-194 as in wild-type iNOSox (17). Gel filtration analysis revealed that seven mutants were mostly or completely monomeric as purified (R375A, F470A, F470Y, W455A, W455F, W455Y, and W457F), whereas two mutants (W457A and F470W) were primarily dimeric (Table I), as is typically observed for wild-type iNOSox purified under identical conditions (17). Overnight incubation of monomer mutants with different concentrations of H4B or with H4B plus Arg converted them to dimers in most but not all cases (Fig. 2, summarized in Table I). In particular, R375A, F470A, and W455A did not dimerize even after overnight incubation with 1 mM H4B and 20 mM Arg. H4B alone (0.5 or 1 mM) promoted dimerization of W455F, W455Y, W457F, and F470Y monomers, whereas Arg alone (20 mM) promoted dimerization of wild-type iNOSox and the mutant monomers F470Y, W455Y, W457A, and W457F but not W455F. Of those mutants that could dimerize, maximum dimerization was typically achieved in the presence of both Arg and H4B. These results indicate that mutation of Arg-375, Phe-470, or Trp-455 to Ala prevented iNOSox from forming a homodimer under any circumstance, whereas mutation of Trp-457 to Ala, or mutations that preserved the aromatic character of Phe-470, Trp-455, and Trp-457, did not prevent homodimer formation in response to H4B and Arg.

All mutant proteins bound DTT to form a ferric bisthiolate complex with characteristic split Soret band at 380 and 460 nm (data not shown), as occurs for wild-type iNOSox dimer in the absence of Arg and H4B (17). When BME replaced DTT as the buffer thiol, the mutants all displayed a Soret absorbance at 415 nm indicating low spin ferric heme iron, as occurs for wild-type iNOSox under these conditions (17). In general, mutants that were dimeric as isolated, or mutant monomers that could form a dimer in response to incubation with H4B and 20 mM Arg, displayed spectral shifts in their Soret bands toward high spin when incubated overnight with H4B plus Arg (Fig. 3, *A–D*), as observed for wild-type iNOSox (17). Incubation of these mutants with H4B or Arg alone caused variable conversion to high spin (Fig. 3). For mutants that were monomeric as isolated, the spectral changes obtained correlated with the amount of dimerization achieved under each incubation condition. Mutants that could not dimerize in response to Arg alone (W455F) or in response to H4B plus Arg (R375A, F470A, and W455A) showed no spectral change after overnight incubation with Arg and H4B, consistent with iNOSox monomer being unable to bind these molecules (22, 25). These spectral results suggest that all mutant homodimers underwent relatively normal changes in their heme iron ligand environment upon binding H4B and Arg.

Arg binding affinities of iNOSox mutant homodimers were quantitated by spectral perturbation assay (17, 39). Spectral change *versus* increasing Arg concentration was recorded in the presence or absence of 0.4 mM imidazole and H4B. In all cases, protein samples were preincubated overnight with 0.5 or 1 mM H4B, and these H4B concentrations were maintained after diluting the enzyme for Arg titration. The spectral change observed for each mutant upon addition of 0.4 mM imidazole indicated its binding to the heme iron was complete at this concentration. To aid in comparing apparent K_s values for Arg, imidazole titrations were performed on select proteins and gave estimated imidazole K_s values of 56 μM for wild-type iNOSox and 50, 31, and 23 μM for F470Y, F470W, and W457F mutants, respectively.

Upon sequential addition of Arg, we obtained spectral changes that indicated a complete displacement of imidazole only for wild-type iNOSox and the F470Y and F470W mutants (F470W is shown in Fig. 4). The apparent Arg K_s values for these two mutants in the presence of 0.4 mM imidazole were derived by double-reciprocal analysis and were 26 and 50 μM, respectively, as compared with 25 μM for wild-type iNOSox under the same conditions (Table I). When each protein's different imidazole affinity is taken into account, corrected Arg K_s values for the F470Y and F470W mutants were 2.9 and 3.6 μM, respectively, similar to the corrected Arg K_s for wild-type iNOSox (3.1 μM).

Other mutant homodimers either achieved an incomplete displacement of imidazole at Arg saturation (W457F, Fig. 4), or exhibited no displacement of imidazole (W455Y, W455F, and W457A) even at Arg concentrations up to 50 mM (data not shown). In these cases, Arg spectral perturbation was measured in the absence of imidazole. W455F, W455Y, and W457F completely converted to high spin during Arg titration in the absence of imidazole and had estimated K_s values between 80 and 150 μM (W455Y titration is shown in Fig. 4, all K_s values are in Table I). The W457A mutant dimer was unstable over the course of the Arg titration, and consequently its K_s value could not be determined.[4] Together, our results indicate that Arg can bind to all mutant homodimers, and their effect on Arg affinity ranges from none to a decrease by less than a factor of 10.

[4] The protein was unstable at room temperature. However, it became fully high spin when incubated overnight with Arg and H4B at 4 °C (see Fig. 2*D*).

TABLE I
Properties of iNOSox mutants

The iNOS ox proteins were incubated overnight at 4 °C in the presence of the indicated concentrations of H4B and Arg and then diluted for activity assays, gel filtration, spectral measurements, and heterodimer experiments as detailed under "Experimental Procedures" and "Results." NA, not applicable; UD, undetermined.

iNOSox protein	Added H4B	Added Arg	Dimer[a]	Homodimer activity[b]	EC_{50} H4B[c]	Ks Arg[d,e]	Imidazole displacement[f]	Heterodimer activity[g]	Antagonist[h]
	mM	mM	%	%	μM	μM		%	
Wild type	0.01	0	>90	100	1.3 ± 0.8	25[d], 16[e]	Complete	100	NA
F470A	0	0	<10					40 ± 5	Complete
	0.5	0	<10						
	1	0	<10						
	1	20	<10						
	0	20	<10						
F470Y	0	0	<10					105 ± 5	NA
	0.5	0	80						
	1	0	80	75 ± 6	3.3 ± 0.5	26[d]	Complete		
	1	20	90						
	0	20	60						
F470W	0	0	60					92 ± 5	NA
	0.5	0	80						
	1	0	80	53 ± 7	7.5 ± 0.7	51[d]	Complete		
	1	20	80						
	0	20	60						
W457A	0	0	60					12 ± 2	Complete
	0.5	0	70						
	1	0	70	10	UD	UD	None		
	1	20	80						
	0	20	70						
W457F	0	0	<10					30 ± 5	Complete
	0.5	0	50						
	1	0	70	66 ± 4	12 ± 3	96[e]	Partial		
	1	20	80						
	0	20	60						
W455A	0	0	<10					10 ± 2	Poor
	0.5	0	<10						
	1	0	<10						
	1	20	<10						
	0	20	<10						
W455F	0	0	<10					30 ± 5	Complete
	0.5	0	<10						
	1	0	50	33 ± 5	16 ± 3	150[e]	None		
	1	20	70						
	0	20	<10						
W455Y	0	0	<10					60 ± 4	Complete
	0.5	0	50						
	1	0	70	36 ± 5	10 ± 2	82[e]	None		
	1	20	90						
	0	20	60						
R375A	0	0	<10					25 ± 5	Complete
	0.5	0	<10						
	1	0	<10						
	1	20	<10						
	0	20	<10						

[a] Estimated by gel filtration chromatography, two runs.
[b] Activity relative to wild-type in the H_2O_2-driven NOHA oxidation assay after overnight incubation with 1 mM H4B. Mean ± S.D. of three separate experiments, each in triplicate.
[c] Estimated from data in Fig. 5. Mean ± S.D. for three separate experiments, each in triplicate.
[d] Determined spectrally in the presence of 0.4 mM imidazole. Mean of two experiments.
[e] Determined spectrally in the absence of imidazole. Mean of two experiments.
[f] Determined by spectroscopic Arg titration.
[g] Derived from maximum values in Fig. 8. Mean ± S.D. for two separate experiments, each in triplicate.
[h] Complete antagonists were able to displace completely wild-type iNOSox monomers in forming a G450A heterodimer (see Fig. 8).

We next examined the ability of each mutant homodimer to catalyze nitrite formation from NOHA in a 10-min H_2O_2-supported reaction (16). This assay directly measures activity of oxygenase domain homodimers because it does not require electron donation from an iNOS reductase domain. Each concentrated wild-type and mutant iNOSox (20–80 μM) was incubated overnight with 1 mM H4B. The next day the dimer-monomer ratio of each sample was determined by gel filtration (see Table I), and the proteins were diluted to 150 nM in the wells and assayed immediately in the presence of 1 mM NOHA and increasing H4B concentrations. H4B carryover from the overnight incubations ranged from 2 to 8 μM. As shown in Fig.

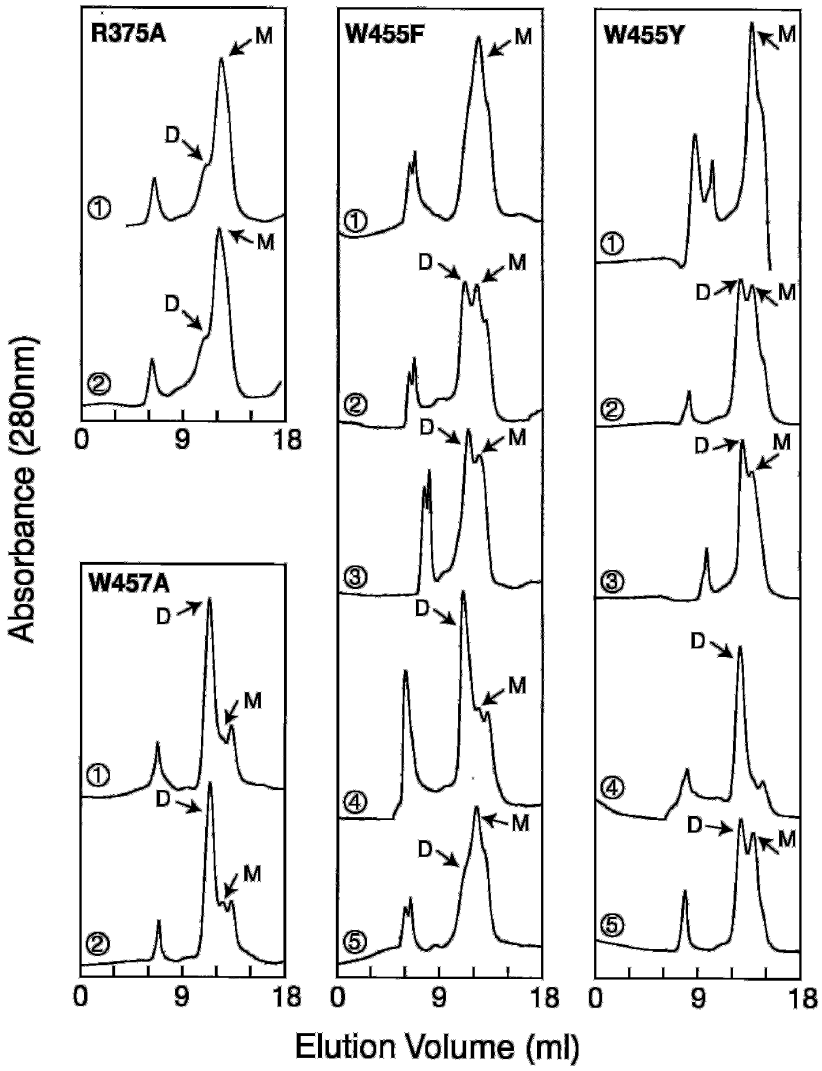

FIG. 2. **Effect of H4B or Arg on monomer-dimer equilibrium of select iNOSox mutants.** Gel filtration profiles were obtained for mutants in the absence of H4B and Arg or after incubating the mutants overnight at 4 °C with various concentrations of H4B and Arg. *A* and *D* contain profiles of R375A and W457A iNOSox mutants, respectively, in the absence of H4B and Arg (*1*) or after incubation with 1 mM H4B plus 20 mM Arg (*2*). *B* and *C* contain profiles of W455F and W455Y iNOSox mutants, respectively, in the absence of H4B and Arg (*1*), or after incubating overnight with 0.5 mM H4B (*2*), 1 mM H4B (*3*), 20 mM Arg (*5*), or 1 mM H4B plus 20 mM Arg (*4*). Dimer (*D*) and monomer (*M*) peaks are indicated by *arrows* and were identified based on retention times for protein molecular weight standards and wild-type iNOSox.

5, all mutants except W457A showed increasing activity as the H4B concentration increased. Table I contains the estimated H4B EC_{50} values derived from this experiment which ranged from 3 to 16 μM, as compared with an EC_{50} value for wild-type iNOSox of 1.3 μM derived from the same assay.

Because the activity of the W457A mutant did not increase with increasing H4B concentration, we used spectroscopy to check if H4B and NOHA bound to W457A under the conditions of the H_2O_2 assay. As shown in Fig. 6, adding 0.1 mM H4B plus 1 mM NOHA completely displaced DTT from the W457A heme iron, indicating saturation of their binding sites was achieved under the assay conditions.

Mutant proteins incubated overnight with 1 mM H4B achieved only partial dimerization in most cases (see Table I). Therefore, activities of the mutants as illustrated in Fig. 5 could not be compared directly without first normalizing for dimer content. When their different dimerization is taken into account (see Table I), the W457A mutant homodimer had the lowest activity compared with wild-type iNOSox, mutant dimers F470W, W455Y, and W455F had activities that ranged from 51 to 66% of wild-type, and mutant dimers F470Y and W457F had activities equivalent to wild-type in the H_2O_2-driven NOHA oxidation assay.

We next examined how each mutation would affect catalytic function when it was present in only one oxygenase domain subunit of an iNOS heterodimer. Our previous work (22, 23) had shown that in a heterodimer comprised of one full-length and one oxygenase domain subunit, the single reductase domain transfers electrons only to the adjacent oxygenase domain partner, and this intersubunit electron transfer supports a full rate of NO synthesis by that oxygenase domain. To make heterodimers using our mutant iNOSox proteins, they were converted to monomers by dissociation in urea, diluted, and incubated with full-length iNOS monomer under conditions that induce dimerization (H4B plus Arg), and finally assayed for NO synthesis in a subsequent 60-min reaction. In this system we used a full-length iNOS monomer containing a point mutation (G450A) that prevents it from forming a homodimer with itself but allows it to form an active homodimer with either wild-type iNOSox monomer or with iNOSox monomers that contain mutations distinct from G450A (18, 42). Thus, we studied the ability of each iNOSox point mutant to "complement" the G450A iNOS monomer regarding heterodimer formation and NO synthesis. We also tested the ability of each mutant to compete with or "antagonize" wild-type iNOSox monomer in forming a heterodimer with G450A iNOS, as a measure of the mutants affinity toward the G450A subunit. The complementation and antagonism experimental methods are illustrated in Fig. 7.

Fig. 8*A* shows results obtained in G450A complementation studies using wild-type iNOSox, three Phe-470 mutants (Tyr, Trp, and Ala), and the R375A mutant. When increasing quantities of wild-type iNOSox monomer were incubated with a constant amount of full-length G450A under dimerization con-

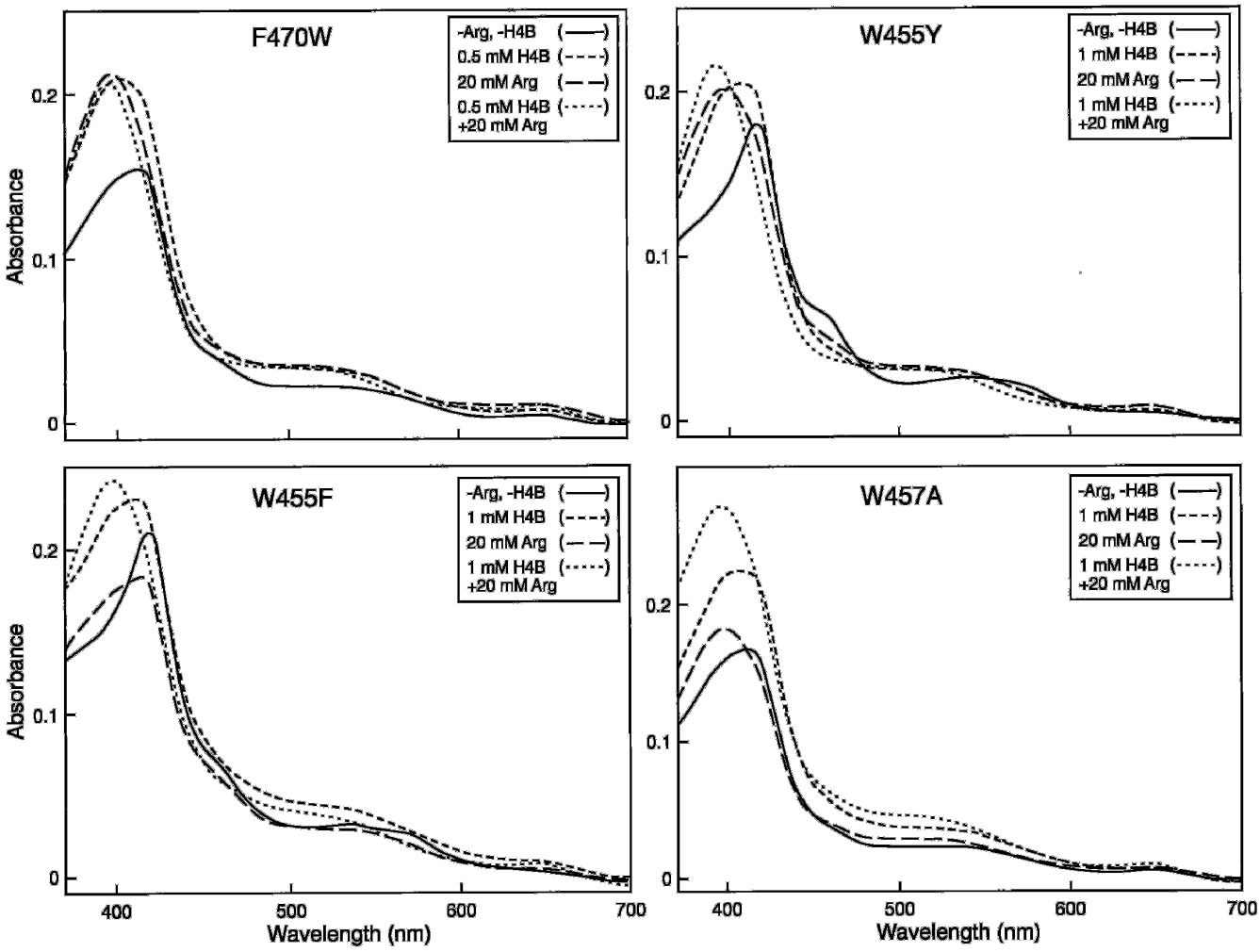

FIG. 3. **Light absorbance spectra of select iNOSox mutants.** Spectra were recorded for mutant proteins after dilution in buffer containing 3 mM BME alone (*-Arg, -H4B*) or after incubating the mutant proteins overnight at 4 °C in buffer containing BME plus various combinations of Arg or H4B as indicated. Spectra were recorded at 15 °C.

ditions, we observed a dose-dependent increase in NO synthesis activity that approached saturation at higher iNOSox to G450A subunit ratios. This indicated heterodimer formation had occurred. The maximal specific activity achieved (477 nmol of NO per min per mg of Gly-450 hemeprotein), as measured by the oxyhemoglobin assay, is similar to the activity of an iNOS heterodimer comprised of wild-type full-length and oxygenase iNOS subunits assayed under similar conditions (~400 nmol NO per min per mg) (22). This indicates that all of the G450A subunits in the reaction formed a heterodimer when excess iNOSox monomers were present and that this heterodimer has normal activity. Experiments utilizing F470Y or F470W iNOSox monomers in place of wild-type iNOSox gave activity *versus* concentration curves almost identical to wild-type iNOSox (Fig. 8*A*). Thus, these two mutations do not affect NADPH-dependent NO synthesis by the heterodimer. In contrast, the F470A and R375A iNOSox monomers achieved maximum heterodimer NO synthesis activities that were 40 and 25% the activity obtained with wild-type iNOSox, respectively. This suggests that the F470A or R375A mutations impact negatively on NO synthesis when they are present in the active oxygenase subunit of the heterodimer.

We also examined the ability of the F470Y, F470A, and R375A mutant iNOSox monomers to compete with a fixed amount of wild-type iNOSox in forming a heterodimer with G450A (Fig. 8*B*). This antagonism study showed that increasing concentrations of F470Y iNOSox did not affect the NO synthesis activity of the system, consistent with the F470Y mutant forming a heterodimer whose activity is equivalent to a heterodimer formed with wild-type iNOSox (see Fig. 8*A*). In contrast, adding increasing amounts of the F470A or R375A monomers in the antagonism study lowered heterodimer NO synthesis activity in a concentration-dependent manner down to levels that were equivalent to the maximum activities obtained for each mutant's complementation assay in Fig. 8*A*. Thus, excess F470A and R375A monomers could compete successfully and completely with wild-type iNOSox monomer in forming a heterodimer with the G450A subunit. This indicated a good affinity toward the G450A subunit and confirmed that heterodimers containing a F470A or R375A subunit possess a lower activity than wild type.

Similar G450A complementation and antagonism experiments were performed with the W457F or W457A monomers (Fig. 8, *C* and *D*) and with the W455A, W455Y, or W455F monomers (Fig. 8, *E* and *F*). Heterodimers containing a W457F or W457A iNOSox subunits were only 12 or 28% as active as a heterodimer containing wild-type iNOSox, whereas heterodimers containing W455Y or W455F iNOSox subunits were 70 and 45% as active as wild type, respectively. All mutants except W455A were also complete antagonists. Thus they have good affinity toward the G450A monomer, and their maximal activities accurately reflect how each mutation affects het-

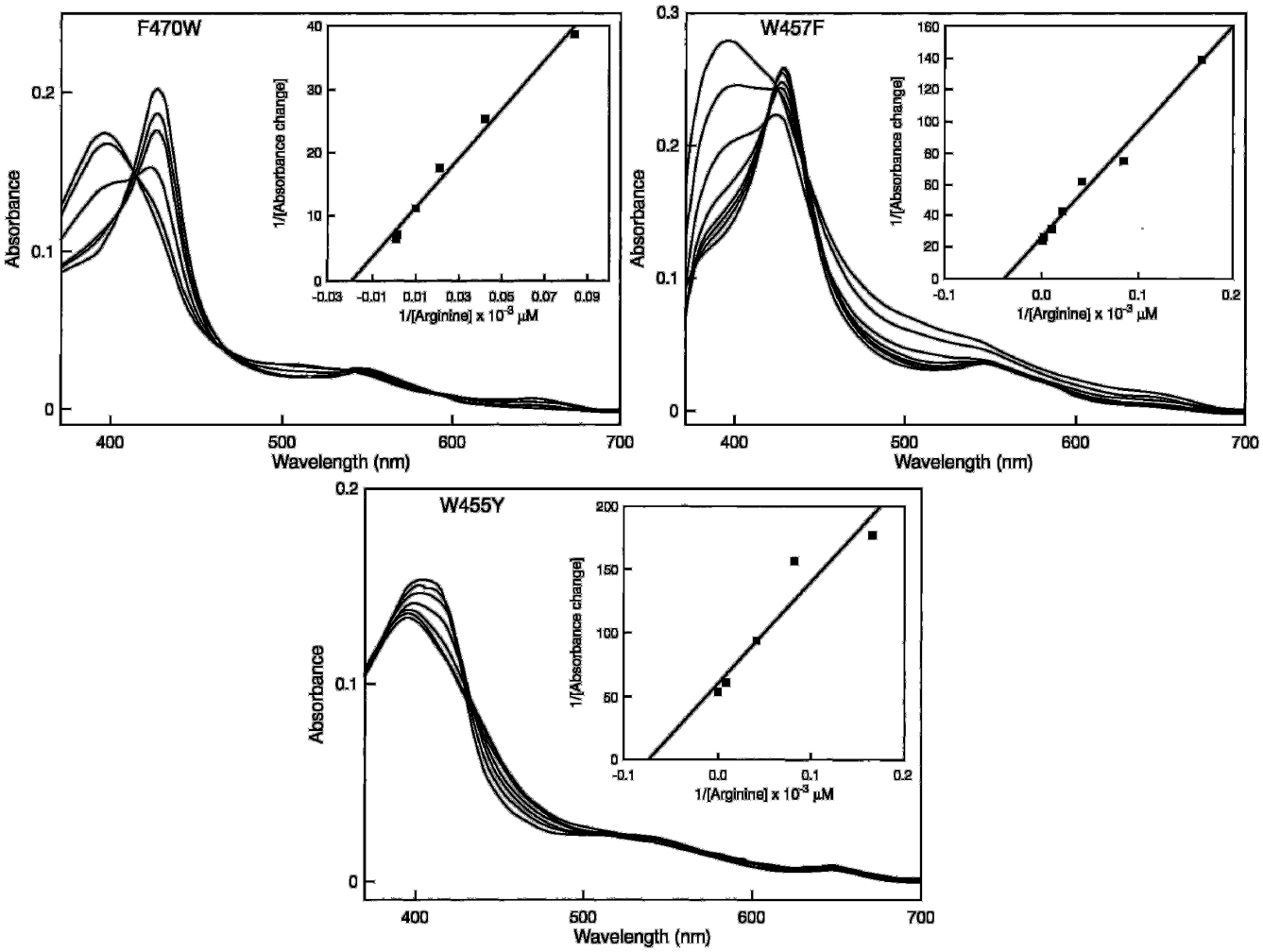

FIG. 4. **Arg binding to mutant proteins as studied by spectral perturbation.** Mutant proteins were diluted in cuvettes containing 40 mM EPPS buffer, pH 7.6, containing 5% glycerol (v/v) and 2 mM BME, 1 mM H4B, and in some cases 400 μM imidazole (F470W and W457F). Light absorbance spectra were recorded at 15 °C prior to and 10 min after each sequential addition of concentrated Arg solution. Final Arg concentrations ranged from 5 μM to 10 mM. The final trace shown in each panel is one at which addition of more Arg caused no further change. The *insets* contain reciprocal plots of absorbance change *versus* Arg concentration used to estimate the apparent binding constant for Arg in each circumstance.

erodimer NO synthesis V_{max}. In contrast, the poor ability of the W455A monomer to antagonize heterodimer formation between G450A and wild-type iNOSox subunits suggests the low activity of the W455A heterodimer (Fig. 8*E*) is primarily due to a dimerization defect.

The relative maximal activities of the mutant heterodimers as shown in Fig. 8 were independently checked by assaying for NO synthesis using the oxyhemoglobin assay. Heterodimers were formed in reactions that contained a 10 to 1 ratio of iNOSox mutant monomer to G450A monomer. As shown in Table II, the NO synthesis activities of the heterodimers had a similar rank order to the activities as measured by the nitrite accumulation assay, confirming that certain mutations substantially decreased NO synthesis activity when present in the active subunit of an iNOS heterodimer.

DISCUSSION

NOSs are the only heme-containing enzymes known to require a pterin cofactor for activity. The influence of H4B on NOS structure and catalysis is complex and may differ among the NOS isoforms (4, 11, 12, 35). Here we utilized mutagenesis to investigate how four conserved residues that interact primarily with the H4B ring help modulate its function in iNOS.

Mutagenesis of these four residues produced a range of effects including destabilization of iNOSox homodimeric structure, reduced binding affinity toward H4B and substrate, changes in heme environment, and reduced rates of NO synthesis. However, no mutations destabilized heme incorporation or its proper ligation with Cys-194, despite several mutants being expressed as heme-containing monomers. This indicates that none of the point mutations perturbed iNOSox folding to form a monomer or its overall structure. Mutation results for each of the four residues is discussed in turn below, followed by a more general discussion.

Arg-375 is located on the substrate binding helix α7a (Fig. 1*A*), which participates in an extensive hydrogen bond network involving charged residues of the α7 helix. It interacts with an H4B molecule bound within the same subunit exclusively through its guanidine nitrogens, which hydrogen-bond directly to pterin O-4 and indirectly to pterin N-5 via a water molecule (Fig. 1*C*). The carboxylate of Asp-379, also found on α7a, hydrogen-bonds to the Arg-375 guanidinium group and positions Arg-375 to serve as a book end for the stacking of H4B with Trp-457. Thus, substitution of Arg-375 to Ala will disrupt π-stacking, hydrogen bond interactions, and electrostatic complementarity in the iNOS dimer.

Because Arg-375 is a central structural residue for the H4B-binding site, the active center, and the dimer interface, it is not surprising that R375A mutants are isolated primarily as mono-

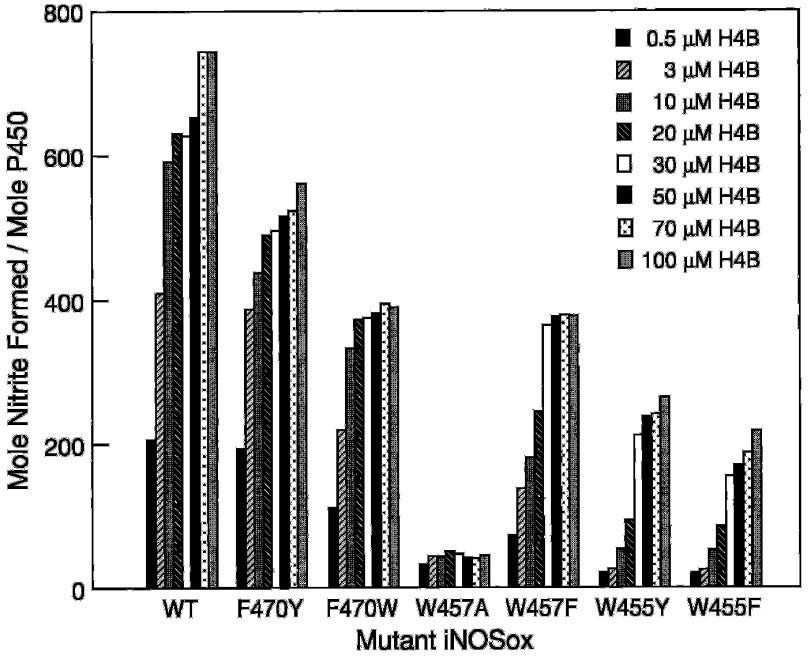

FIG. 5. **Activity of iNOSox mutants as a function of H4B concentration.** Activity was measured as nitrite formed from NOHA in a 10-min H_2O_2-dependent assay run at 37 °C. Mutant proteins were incubated overnight at 4 °C with 0.1 mM H4B prior to assay. Assays were performed as indicated under "Experimental Procedures" and contained 150 nM hemeprotein, the indicated concentrations of H4B and 1 mM NOHA, and were initiated by adding H_2O_2. The values shown are the mean of three independent experiments.

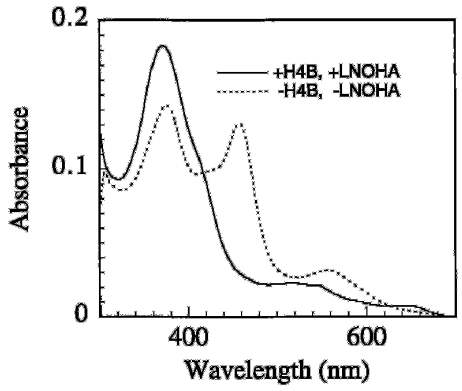

FIG. 6. **Spectral analysis of H4B binding to W457A iNOSox.** The mutant was diluted in buffer containing 3 mM DTT and a spectrum recorded. NOHA and H4B were added, and another spectrum was recorded after 10 min.

mers that do not form a homodimer in response to H4B or Arg. The minor amount of dimeric R375A that we observe is likely to have formed through H4B-independent dimerization, which occurs extensively for wild-type iNOS when it is expressed in bacteria (Table I). The inability of R375A to dimerize further in response to H4B or Arg implies that the mutation either prevents their binding to or stabilization of the mutant homodimer. In any case, the R375A monomer clearly formed a heterodimer with a full-length iNOS G450A subunit, which generated NO from Arg at ~25% of the wild-type activity. This shows the following: 1) the R375A subunit can bind H4B and Arg productively when coerced into a dimeric state; and 2) the multiple hydrogen-bonding interactions and positive charge supplied from Arg-375 cannot be absolutely essential for H4B binding or to support NO synthesis but may be needed to optimize binding affinity, dimerization, and catalysis by iNOS.

As noted by Raman *et al.* (24) ricin also recognizes pteridine-based inhibitors with an Arg residue that interacts with O-4 of the pterin ring (43), whereas in dihydropteroate synthase a positively charged Lys recognizes pterin rings at O-4 (44). Perhaps the closest analogy to iNOS Arg-375 occurs in dimethyl sulfoxide reductase, where an Arg is positioned in a conformation similar to iNOS Arg-375 and hydrogen-bonds to an O-4 equivalent on the molybdopterin cofactor (45, 46). However, the roles of pterin and overall structures of the binding sites are very different in all of these enzymes. This implies that hydrogen bonding between pterin O-4 and a positively charged residue does not confer specific chemical or electronic functionality on H4B but rather enables proper binding of the cofactor. Interestingly, mutation of the analogous Arg residue in human eNOS (R365L), which hydrogen-bonds to the O-4 of H4B as in iNOS, did not completely prevent eNOS homodimer formation as judged by the mutant possessing considerable citrulline synthesis activity (47). This suggests that differences exist among NOS isoforms regarding a role for this Arg residue in H4B binding and function.

The H4B-binding sites of iNOS and eNOS are distinguished by a high degree of aromatic character primarily provided in iNOS by Trp-455, Trp-457, Phe-470, and the H4B ring itself. Of these residues, Trp-457 is located on the helical lariat and interacts with an H4B that is contained within the same subunit. The indole ring of Trp-457 is involved in an extensive π-stacking arrangement that also includes Phe-470 from the partner subunit (Fig. 9). The indole ring is sandwiched between H4B's ring and the guanidinium of Arg-193, which is probably involved in a favorable interaction with the quadrupole of the indole ring. One end of the Trp-457 indole ring lies between the A and D pyrrole rings of the heme, whereas the other is contacted by Met-114 (Fig. 9), which is located in the amino-terminal H4B-binding segment (19). Trp-457 also forms hydrogen bonds between its α-carbonyl and the N-2 and N-1 nitrogens of the H4B ring (Fig. 1C). In addition, the indole NH hydrogen bonds to a water molecule that interacts with the terminal hydroxyl group of the chain of H4B.

The W457F mutant is predicted to conserve the aromatic stacking and backbone hydrogen-bonding interactions with H4B, whereas the W457A mutation should only conserve hydrogen-bonding between the ring nitrogens of H4B and the peptide backbone. Surprisingly, substitution of Trp-457 to Ala did not significantly destabilize the dimeric structure in the as-isolated protein, whereas substitution to Phe did, even though the W457F mutant still dimerized in the presence of H4B or Arg. Both mutants readily formed heterodimers with a full-length G450A subunit and acted as good antagonists. This indicates that π-stacking of Trp-457 with H4B may have only a minor role in stabilizing the dimeric structure and that it is

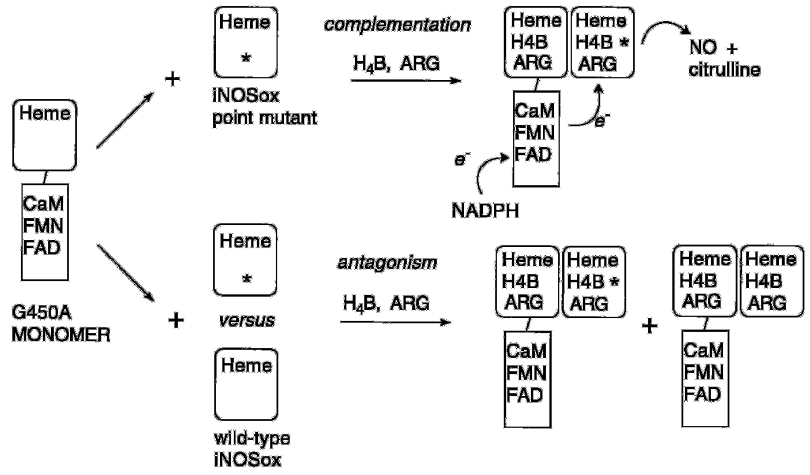

FIG. 7. **G450A complementation and antagonism methods used to characterize iNOSox mutants.** In the complementation assay, wells contain different amounts of an iNOSox mutant monomer (denoted with a *star*) plus a constant amount of G450A monomer. Dimerization is promoted by incubation with H4B and Arg. Heterodimer NO synthesis is then assayed in the NADPH-driven Arg oxidation assay. As shown, electrons are transferred only to the heme of the mutant oxygenase subunit and not to the heme of the G450A subunit. The antagonism assay is carried out in an identical manner except that the wells also contain a constant amount of wild-type iNOSox monomer, which competes with the mutant iNOSox monomer in forming a heterodimer with the G450A subunit.

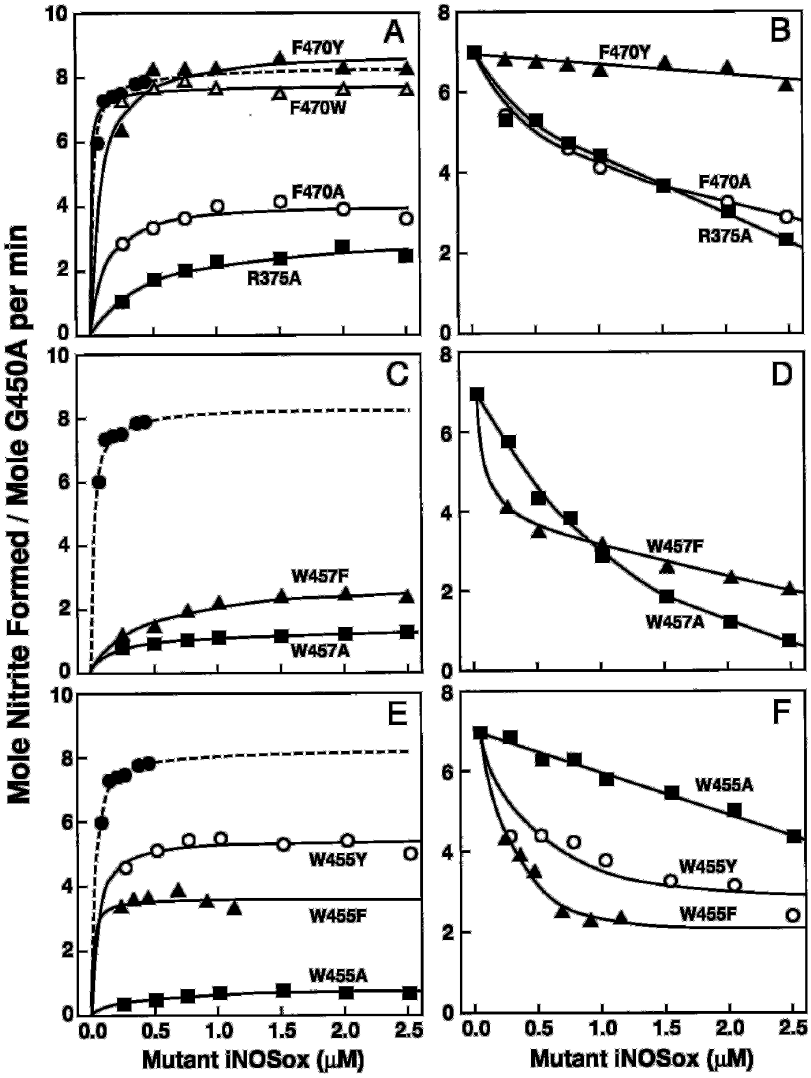

FIG. 8. **Mutant activities in G450A heterodimer complementation and antagonism assays.** *A, C,* and *E* are complementation studies done with the indicated mutants and with wild-type iNOSox monomer (- - -) included for comparison. *B, D,* and *F* are antagonism studies done with the indicated mutants. All assays measured nitrite produced from Arg in a NADPH-driven reaction. The *solid lines* are computer-derived curves of best fit using the equation $y = ax/(b + x)$ for complementation data, and the equations $y = mx + b$ or $y = ae^{-bx} + ce^{-dx} + f$ for antagonism data. See Fig. 7 and "Experimental Procedures" for additional details.

more detrimental structurally to replace Trp-457 with an aromatic of different size than to remove it completely. However, maintaining the stacking interaction may be critical for controlling heme environment and reactivity, as manifested by the inability of Arg to displace heme-bound imidazole in the W457A mutant and its lower rate of catalysis in both the H_2O_2-driven NOHA oxidation and heterodimer NO synthesis assays. Because our spectral results show that W457A was able to fully bind H4B and substrate under the conditions of the catalytic assay (see Fig. 6), we can conclude its diminished activities are not related to poor binding of substrate and cofactor. Likewise, its low activities cannot be explained by poor dimerization (see Table I). Thus, Trp-457 must have an important direct role that helps H4B to support NO synthesis. Possibilities to investigate include the effect of H4B on heme iron reduction (35), heme iron-oxy reactivity (32), and formation or stabilization of a heme-NO complex during steady-state NO synthesis (48, 49).

W457F, which potentially preserves a stacking interaction with H4B, displayed relatively normal spectral properties although imidazole displacement by Arg was incomplete. This mutant's rate of NOHA oxidation in the H_2O_2-driven assay was normal, but it was only 30% as active as wild-type in the heterodimer NO synthesis assay. This suggests aromatic substitution at Trp-457 does not alter heme catalytic activity in the simpler assay system, but maintaining Trp at position 457 is important for NO synthesis from Arg, which is a much more complex reaction.

Each H4B-binding site in NOS is comprised of residues supplied from both subunits. In addition, several structural interactions occur between the helical lariats of the two subunits that couple the H4B-binding sites together within the dimer interface (19). Phe-470 and Trp-455, which are positioned on the helical lariat, contact the H4B molecule that is bound in the adjacent subunit. In the crystal structure Phe-470 and Trp-455 stack against the H4B ring on the side opposite to Trp-457, with the Phe-470 ring tilted to complement the tetrahydropyrazine ring pucker and (6*R*)-dihydroxypropyl side chain projection (see Figs. 1*A* and 9). The backbone carbonyl of Phe-470 hydrogen-bonds with H4B side chain hydroxyl O-9 and the phenyl ring also contacts Ser-465 and His-471 of the same subunit. In addition, Phe-470 buries ~55-A^2 in the dimer interface by contacting Trp-455 and Pro-461 of the adjacent subunit. Phe-470 is further stabilized by a hydrogen bond between its peptide carbonyl and the indole nitrogen of Trp-455. Trp-455 itself contacts the H4B side chain and stabilizes conformations for Ile-456 and Val-459 of the adjacent subunit. This residue buries 70 A^2 in the dimer interface, primarily by stacking with its own symmetry mate (Trp-455) on the adjacent subunit. Thus, in addition to their H4B contacts, Phe-470 and Trp-455 have multiple interactions with residues from both subunits and are integral components of the dimer interface.

TABLE II
NO synthesis activities of various G450A mutant heterodimers

NO synthesis activities were determined using the oxyhemoglobin spectrophotometric assay. Activity values represent nanomoles of NO produced per min per mg of G450A hemeprotein at 37 °C and are the mean of two measurements each.

iNOSox subunit	Heterodimer-specific activity
Wild type	477
F470Y	611
F470W	492
W455Y	325
W455F	196
F470A	65
W455A	46
W457A	<10
R375A	<10

Aromatic substitution mutations of Phe-470 and Trp-455 altered dimer stability and substrate- or H4B-protein interactions to various degrees but never completely prevented dimer formation, binding of H4B and substrate, or NO synthesis. Only substitution at Trp-455 altered the iNOS heme environment as judged by an inability of Arg to displace heme-bound imidazole. Aromatic substitution at Phe-470 had either a minor or no effect on catalysis as measured in the H_2O_2-driven NOHA oxidation or heterodimer NO synthesis assays, whereas aromatic substitution at Trp-455 decreased activity in both activity assays. Ala substitution at Phe-470 completely prevented homodimer formation, but this mutant still formed a heterodimer with a full-length G450A subunit which had significant NO synthesis activity. In contrast, Ala substitution at Trp-455 completely prevented homodimerization and almost completely prevented formation of the G450A heterodimer, in this way severely diminishing NO synthesis.

Together, our results suggest a proper stacking interaction between Phe-470 and H4B can be provided by other aromatic residues, and thus the precise interaction supplied by Phe-470 is not critical. In contrast, altering the stacking and protein hydrogen-bonding interactions of Trp-455 have a greater and broad effect on iNOS structure and catalysis that may involve both subunits of the iNOS dimer. Indeed, although it is clear that mutations of Phe-470 and Trp-455 should affect H4B binding or function in the opposite subunit, the extensive structural integration of the two H4B sites and participation of Trp-455 residues from both subunits in forming the dimer interface help explain why the W455F and W455Y heterodimers had lower rates of NO synthesis even when the mutations were located in the same subunit as the active heme.

Although Arg-375, Trp-455, Trp-457, and Phe-470 each appear important for H4B functions in iNOS, our results reveal that NO synthesis does not absolutely depend on preserving the individual identities of any of these four residues. Thus,

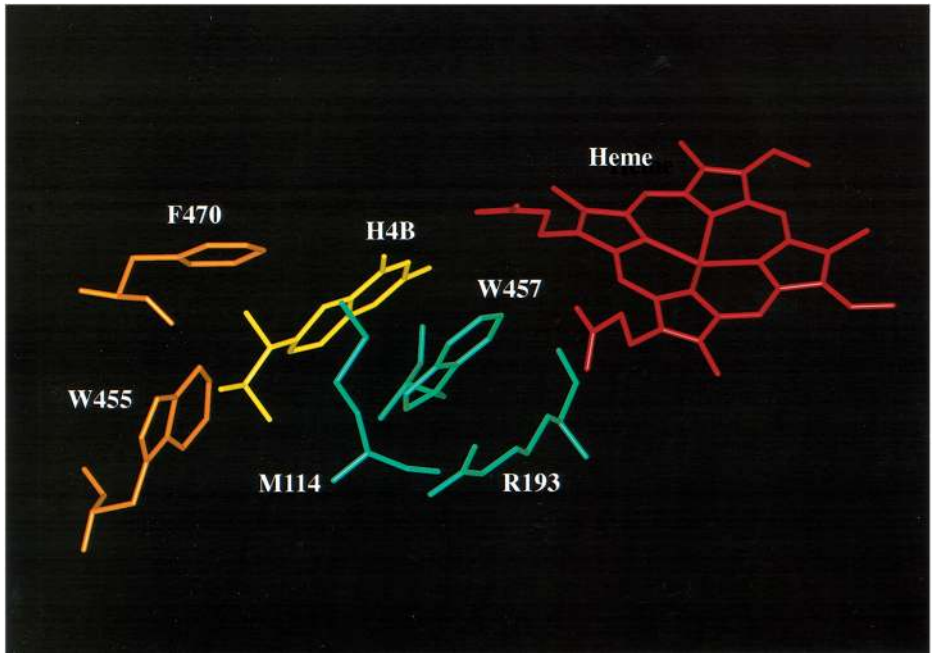

FIG. 9. **Interactions among the conserved aromatic residues that make up the H4B-binding site.** *Green* residues are provided by the same iNOSox subunit in which the H4B (*yellow*) is bound, and *orange* residues are provided by the partner subunit of the dimer.

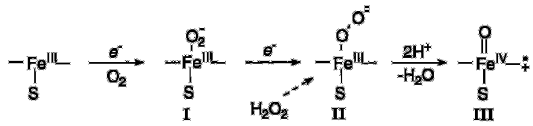

FIG. 10. **Possible oxygen activation pathways in iNOS.** An electron ($e-$) provided by the iNOS reductase domain enables ferrous heme to bind O_2 and form species I. Provision of a second electron enables formation of species II, which can cleave in a proton-assisted reaction to form species III, which is depicted as an iron-oxo heme cation radical. H_2O_2 can bind directly to form species II, eliminating a need for reductase domain electrons.

none of their functional group interactions with H4B or with other protein residues are absolutely critical. It is important to note that this conclusion could only be reached by virtue of heterodimer experiments, which allowed us to determine how mutations that completely prevented iNOS homodimer formation (most Ala mutants) affect iNOS catalysis in a dimeric setting.

A body of evidence suggests that many mutations limit or prevent iNOS NO synthesis primarily by limiting homodimer formation. Known mutations that completely prevent iNOS homodimer formation (and consequent NO synthesis) include certain amino-terminal deletion mutants (17), point mutants G450A and A453I (42), and three of the four Ala mutants described in the present report. In principle, this mechanism of inhibition also applies for any mutant that has a partial dimeric structure under a given experimental setting because H4B or Arg concentrations were insufficient for full dimer formation (16, 17). Our work shows that provision of sufficient H4B and Arg, and heterodimer experiments, can often circumvent dimerization defects and thereby allow study of how a given mutation effects NO synthesis by the dimer itself.

Three mutations described in this report (W457A, W455F, and W455Y) altered the iNOS heme environment as judged by an inability of Arg to displace imidazole bound to the heme. Similar effects on heme environment have also been reported for eNOS point mutants (47). For our iNOS mutants, the inability of substrate to displace bound imidazole could not be explained by poor dimerization or lack of Arg or H4B binding. The defect may also be ligand-specific, because in these same mutants Arg could fully displace DTT bound to the heme iron.[5] That mutations in the H4B-binding site can effect Arg-heme ligand interactions is consistent with the iNOS crystal structure that shows Arg binds directly over the heme and an extensive integration exists between the H4B and substrate-binding sites (19). However, because the changes in substrate-heme ligand interactions did not correlate well with loss of catalytic activity in the iNOS mutants, it is presently unclear how they relate to iNOS function.

Mutant activity as measured by the H_2O_2-driven NOHA oxidation assay was usually affected to the same degree or in some cases was less sensitive to a given mutation than was heterodimer NO synthesis. This has potentially important implications. As shown in Fig. 10, the NOS heme is thought to activate oxygen in a stepwise manner with formation of three distinct iron-oxy species. Provision of H_2O_2 to ferric NOS enables formation of heme iron-peroxy species II and potentially formation of the iron-oxo species III and, therefore, bypasses electron transfer and oxygen activation steps that normally occur during NADPH-driven NO synthesis (21, 32, 33). Thus, observing normal activity in the H_2O_2-driven assay implies that a given mutation does not effect formation or reactivity of species II (or potentially species III) toward NOHA. When such mutants display good heterodimer formation but slow heterodimer NO synthesis from Arg, the mutation must either slow the tempo of electron transfer to the heme, alter formation or reactivity of the iron-oxy species toward Arg, or stabilize the inactive heme-NO complex that forms during steady-state NO synthesis. Such changes could explain why aromatic substitution mutants W457F and W455F have slow heterodimer NO synthesis although the π-stacking and hydrogen-bonding interactions of the native residues are largely preserved. Perhaps these facets of catalysis, which are unique to NADPH-dependent NO synthesis from Arg, are more sensitive to the precise positioning or environment provided by these residues. Further work to understand these issues is underway in our laboratories.

It has been proposed that H4B may participate in NOS heme reduction by serving as an intermediate in the electron transfer pathway between the flavins and heme iron (24, 33). Under this circumstance, the quadrupole moments of the aromatic residues surrounding the cofactor might help stabilize an H4B cation radical species formed during an electron transfer event (24, 33). Mutation of aromatic residues contacting H4B could then be envisioned to down-regulate NO synthesis by destabilizing a pterin cation radical and thus modulating the ability of H4B to accept or donate flavin-derived electrons to the heme. Although our data do not formally rule out this possibility, we believe it is unlikely because flavin-dependent heme iron reduction still occurs in both iNOS and nNOS[6] in the absence of bound H4B (29, 35). Moreover, the rate of heme iron reduction in H4B-free iNOS is equal to or slightly faster than the rate in H4B-saturated iNOS (35). This at minimum shows that H4B is not required to achieve a normal rate of flavin-mediated heme iron reduction in NOS. Indeed, our previous data indicate that an essential role of H4B may be to modulate the reactivity of NOS heme iron-oxy complexes that form during NO synthesis (32). In addition, the heme edge in an iNOSox dimer is close to a surface that can interact directly with the reductase domain, whereas H4B is buried in the dimer interface (19) and could only obtain electrons from the reductase by an indirect transfer route.

Comparing all NOS primary sequences available in the data base reveals that the four residues mutated in this report are almost completely conserved across 26 NOS from a wide variety of life forms. The single exception is Trp-457 which in the great pond snail is an Arg (see Fig. 1*B*). Such strict conservation contrasts with our data showing some tolerance toward aromatic substitution with regard to NO synthesis. What selective pressure has maintained residue identities (beyond the fact that some aromatic substitutions would involve a double mutation of the codon) is unclear. Our current data suggest that dimer destabilization or some loss of H4B binding affinity caused by mutation might help maintain selective pressure *in vivo*. Studies that examine assembly and function of the H4B site mutants in whole cells should shed light on this issue.

Acknowledgments—We thank Pam Clark and Pam Mackowski for excellent technical support.

REFERENCES

1. Gross, S. S., and Wolin, M. S. (1995) *Annu. Rev. Physiol.* **57,** 737–769
2. Dawson, T. M., and Dawson, V. L. (1996) *Annu. Rev. Med.* **47,** 219–227
3. Nathan, C. (1997) *J. Clin. Invest.* **100,** 2417–2423
4. Mayer, B., and Werner, E. R. (1995) *Nauyn Schmiedeberg Arch. Pharmacol.* **351,** 453–458
5. Michel, T., and Feron, O. (1997) *J. Clin. Invest.* **100,** 2146–2152
6. Cho, H. J., Xie, Q. W., Calaycay, J., Mumford, R. A., Swiderek, K. M., Lee, T. D., and Nathan, C. (1992) *J. Exp. Med.* **176,** 599–604
7. Garcia-Cardena, G., Martasek, P., Masters, B. S. S., Skidd, P. M., Couet, J., Li, S., Lisanti, M. P., and Sessa, W. C. (1997) *J. Biol. Chem.* **272,** 25437–25440
8. Venema, R. C., Sayegh, H. S., Kent, J. D., and Harrison, D. G. (1996) *J. Biol.*

[5] S. Ghosh and D. J. Stuehr, unpublished results.

[6] In H4B-free iNOS, NADPH-dependent heme reduction requires that Arg or an Arg analog is bound, but this is not required in H4B-free nNOS (29, 35).

Chem. **271,** 6435–6440
9. Griffith, O. W., and Stuehr, D. J. (1995) *Annu. Rev. Physiol.* **57,** 707–736
10. Marletta, M. A. (1993) *J. Biol. Chem.* **268,** 12231–12234
11. Mayer, B., and Hemmens, B. (1997) *Trends Biochem. Sci.* **22,** 477–481
12. Stuehr, D. J. (1997) *Annu. Rev. Pharmacol. Toxicol.* **37,** 339–359
13. Masters, B. S. S., McMillan, K., Sheta, E. A., Nishimura, J. S., Roman, L. J., Martasek, P. (1996) *FASEB J.* **10,** 552–558
14. Abu-Soud, H. M., Wu, C., Ghosh, D. K., and Stuehr, D. J. (1998) *Biochemistry* **37,** 3777–3786
15. Salerno, J. C., Martasek, P., Roman, L. J., and Masters, B. S. S. (1996) *Biochemistry* **35,** 7626–7630
16. Gachhui, R., Ghosh, D. K., Wu, C., Parkinson, J., Crane, B. R., and Stuehr, D. J. (1997) *Biochemistry* **36,** 5097–5103
17. Ghosh, D. K., Wu, C., Pitters, E., Moloney, M., Werner, E. R., Mayer, B., and Stuehr, D. J. (1997) *Biochemistry* **36,** 10609–10619
18. Xie, Q. W., Leung, M., Fuortes, M., Sassa, S., and Nathan, C. (1996) *Proc. Natl. Acad. Sci. U. S. A.* **93,** 4891–4896
19. Crane, B. R., Arvai, A. S., Ghosh, D. K., Wu, C., Getzoff, E. D., Stuehr, D. J., and Tainer, J. A. (1998) *Science* **279,** 2121–2126
20. Ghosh, D. K., Abu-Soud, H. M., and Stuehr, D. J. (1995) *Biochemistry* **34,** 11316–11320
21. Rusche, K. M., Spiering, M. M., and Marletta, M. A. (1998) *Biochemistry* **37,** 15503–15512
22. Siddhanta, U., Wu, C., Abu-Soud, H. M., Zhang, J., Ghosh, D. K., and Stuehr, D. J. (1996) *J. Biol. Chem.* **271,** 7309–7312
23. Siddhanta, U., Presta, A., Fan, B., Wolan, D., Rousseau, D. L., and Stuehr, D. J. (1998) *J. Biol. Chem.* **273,** 18950–18958
24. Raman, C. S., Li, H., Martasek, P., Kral, V., Masters B. S. S., and Poulos, T. M. (1998) *Cell* **95,** 939–950
25. Abu-Soud, H. M., Loftus, M., and Stuehr, D. J. (1995) *Biochemistry* **34,** 11167–11175
26. Renodon, A., Boucher, J. L., Wu, C., Gachhui, R., Sari, M. A., Mansuy, D., and Stuehr, D. J. (1998) *Biochemistry* **37,** 6367–6374
27. Mayer, B., Wu, C., Gorren, A. C., Pfeiffer, S., Schmidt, K., Clark, P., Stuehr, D. J., and Werner, E. R. (1997) *Biochemistry* **36,** 8422–8427
28. Gerber, N. C., Nishida, C. R., and Ortiz de Montellano, P. R. (1997) *Arch. Biochem. Biophys.* **343,** 249–253
29. Presta, A., Weber-Main, A. M., Stankovich, M. T., and Stuehr, D. J. (1998) *J. Am. Chem. Soc.* **120,** 9460–9465
30. Wang, J., Stuehr, D. J., and Rousseau, D. L. (1995) *Biochemistry* **34,** 7080–7087
31. Klatt, P., Schmidt, K., Lehner, D., Glatter, O., Bachinger, H. P., and Mayer, B. (1995) *EMBO J.* **14,** 3687–3695
32. Abu-Soud, H. M., Gachhui, R., Rauschel, F. M., and Stuehr, D. J. (1997) *J. Biol. Chem.* **272,** 17349–17353
33. Bec N., Gorren, A. C. F., Voelker, C., Mayer, B., and Lange, R. (1998) *J. Biol. Chem.* **273,** 13502–13508
34. Rodriguez-Crespo, I., and Ortiz de Montellano, P. R. (1996) *Arch. Biochem. Biophys.* **336,** 151–156
35. Presta, A., Siddhanta, U., Wu, C., Sennequire, N., Huang, L., Abu-Soud, H. M., Erzurum, S., and Stuehr, D. J. (1998) *Biochemistry* **37,** 298–310
36. Wu, C., Zhang, J., Abu-Soud, H. M., Ghosh, D. K., and Stuehr, D. J. (1996) *Biochem. Biophys. Res. Commun.* **222,** 439–444
37. Sambrook, J., Fritsch, E. F., and Maniatis, T. (1989) *Molecular Cloning: A Laboratory Manual,* Cold Spring Harbor Laboratory Press, Plainview, NY
38. Stuehr, D. J., and Ikeda-Saito, M. (1992) *J. Biol. Chem.* **267,** 20547–20550
39. McMillan, K., and Masters, B. S. S. (1993) *Biochemistry* **32,** 9875–9880
40. Ghosh, D. K., Abu-Soud, H. M., and Stuehr, D. J. (1996) *Biochemistry* **35,** 1444–1449
41. Pufahl, R. A., Wishnok, J. S., and Marletta, M. A. (1995) *Biochemistry* **34,** 1930–1941
42. Cho, H. J., Martin, E., Xie, Q. W., Sassa, S., and Nathan, C. (1995) *Proc. Natl. Acad. Sci. U. S. A.* **92,** 11514–11518
43. Yan, X., Hollis, T., Svinth, M., Day, P., Monzingo, A. F., Milne, G. W. A., and Robertus, J. D. (1997) *J. Mol. Biol.* **266,** 1043–1049
44. Hampele, I. C., D'Arcy, A., Dale, G. E., Kostrewa, D., Nielsen, J., Oefner, C., Page, M. G., Schonfeld, H. J., Stuber, D., and Then, R. L. (1997) *J. Mol. Biol.* **268,** 21–30
45. Schindelin, H., Kisker, C., Hilton, J., Rajagopalan, K. V., and Rees, D. C. (1996) *Science* **272,** 1615–1621
46. McAlpine, A. S., McEwan, A. G., Shaw, A. L., and Bailey, S. (1997) *J. Biol. Inorg. Chem.* **2,** 690–701
47. Chen, P.-F., Berka, V., Tsai, A.-L., and Wu, K. W. (1998) *J. Biol. Chem.* **273,** 34164–34170
48. Hurshman, A. R., and Marletta, M. A. (1995) *Biochemistry* **34,** 5627–56311
49. Abu-Soud, H. M., Wang, J., Rousseau, D. L., Fukuto, J., Ignarro, L. J., and Stuehr, D. J. (1995) *J. Biol. Chem.* **270,** 22997–23006
50. Roman, L. J., Sheta, E. A., Martasek, P., Gross, S. S., Liu, Q., and Masters, B. S. S. (1995) *Proc. Natl. Acad. Sci. U. S. A.* **92,** 8428–8432